Physica Scripta

PAPER

Conformal wormholes in $f(R, \mathfrak{L}_m)$ theory

Doğukan Taşer[1], **Melis Ulu Doğru**[2,*], **Erkan Eraslan**[3] and **Hüseyin Aydın**[4]

[1] Department of Electricity and Energy, Çan Vocational School, Çanakkale Onsekiz Mart University, 17400, Çanakkale, Turkey
[2] Department of Physics, Science Faculty, Çanakkale Onsekiz Mart University, 17020, Çanakkale, Turkey
[3] Department of Physics, School of Graduate Studies, Çanakkale Onsekiz Mart University, 17020, Çanakkale, Turkey
[4] State Hydrolic Works (DSI), 61220, Trabzon, Turkey
[*] Author to whom any correspondence should be addressed.

E-mail: dogukantaser@comu.edu.tr, melisulu@comu.edu.tr, erkan.eraslan@comu.edu.tr and huseynaydin@gmail.com

Keywords: exotic fluid, $f(R, \mathfrak{L}_m)$ gravity, conformal symmetry

OPEN ACCESS

RECEIVED
1 February 2024

REVISED
4 June 2024

ACCEPTED FOR PUBLICATION
14 June 2024

PUBLISHED
1 July 2024

Abstract

In this study, we present a new static and conformally symmetric wormhole solution. We develop new wormhole model in $f(R, \mathfrak{L}_m)$ gravity. Shape function of conformally symmetric $f(R, \mathfrak{L}_m)$ wormholes, provided by homothetic vector field is obtained regarding to conformal factor. It is investigated whether the function provides a stable throat infrastructure that does not allow collapsing. Anisotropic fluid matter filled the obtained conformally symmetric traversable wormholes is discussed by examining the dynamical properties of the fluid. Constructed new wormhole model violates all energy conditions. Physical significance of the sources filled constructed wormholes is discussed using volume quantifier. It is revealed that $f(R, \mathfrak{L}_m)$ theory allows traversable and conformally symmetric wormholes if supported by phantom field.

1. Introduction

Studies on investigation of frequency shifts in galaxy spectra, which would inspire future theoretical studies, dates back to early 1900s [1]. So, Friedmann [2] and Lemaitre [3] independently showed that their suggested models, obtained from Einstein field equations, expressed a non-static structure of Universe. Early consistent observational evidences of the dynamical structure were measured by Lundmark [4] and Hubble [5]. Movements of galaxies away from each other were interpreted as Universe becoming larger and expanding. With technological and methodological developments in galaxy observations, expansion constraint is continually renewed [6]. Independent analyzes of calibrated data from different galaxy clusters reveal that constraint of expansion is surprisingly different from initially presented by Hubble [5, 7, 8]. In other words, Universe is not just expanding, it is expanding at an accelerating rate [9]. Local galaxy data from WMAP confirms the findings [10]. An explanation for late-time expansion is interpreted as negative pressure of fluid in a model presented by Friedmann equations [11, 12]. This candidate, called as dark energy, stands for total energy in vacuum state [13]. In the explanation, cosmological constant added to field equations by Einstein to prevent collapse and make Universe static actually represents dark energy. However, particle physics experiments show that observational results of cosmological constant have too different values from those predicted by theory to be acceptable within error tolerance [14]. For this reason, new researches are being developed to replace both Einstein's Theory of General Relativity and dark energy-cosmological constant interpretations. Alternative gravitational theories emerge as another method to explain the expansion. In recent years, while alternative theories and their validities with modifications and/or improvements on Einstein-Hilbert action have been derived. A new and consistent theory approaches, which eliminate problems encountered in Einstein's General Relativity such as not being able to meet quantum nature, being inadequate at high energy limits, incompatibilities of Mach's Principle, normalization problems and not being able to explain early expansion at the same time, gave rise to many exciting proposals. Recently, many studies on scalar field supported scalar-tensor theories [15–17], f(R)-class theories [18–21], k-essence type theories suitable for high energy structures [22], and hybrid structures where these are considered together [23] have been put forward.

A recent popular alternative gravitational theory is $f(R, \mathfrak{L}_m)$ gravity, proposed by Harko and Lobo [24]. In this theory, not only Ricci scalar but also Lagrangian density originating from matter, directly affects action integral for geometry of space-time. Thus, extra forces acting on massive test particles are orthogonal to four-velocities [25]. Massive test particles do not move through the geodesics. This situation can be understood by covariant divergence of energy-momentum tensor being different from zero. Therefore, equivalence principle may not be satisfied in $f(R, \mathfrak{L}_m)$ theory [25]. The scope of the principle, which must be ensured in accordance with solar system tests, is a research topic that has attracted attention in recent years. Some observation data obtained recently from outside the solar system have indicated that the equivalence principle may not be met. The absence of movement along geodesic curves can also explain dark energy, which is held responsible for the expansion of the Universe [25]. $f(R, \mathfrak{L}_m)$ gravity can be considered as a generalization of all alternative gravity theories using Riemannian geometry. Within the scope of theory, cosmological constraints were calculated for non-linear models and expansion scenarios were discussed using redshift data [26]. Also, it is shown that constructed model has quintessence structure [26]. The compatibility of the theory with solar system tests and the equivalence principle was investigated [27]. General energy conditions were defined and also discussed whether they were met or not [28]. The behavior of deceleration, Hubble and density parameters in the case of a massive source was revealed [29]. Radiation dominant period and nucleosynthesis research were given [30]. In addition, traversability of static wormholes in linear and non-linear cases [31], shape function behavior of Morris-Thorne wormholes [32] and stability conditions of Lorentzian wormholes in anisotropic and isotropic cases were examined [33].

As is known, a black hole has singularity at the center. To create a model, free of the singularity, Einstein and Rosen took transformation of reference frame into account in the Schwarzschild solution [34]. The resulting model has a throat around $z(r) \rightarrow 0$ and two separate mouths on the edges of the throat, which are projected onto two different manifolds [35]. The model structure is a tube-like structure that is narrow in the throat and widens in the mouths [36]. Theoretically, the manifolds where the mouths are located can be different regions of the same space-time, or they can be different regions of different universes [37]. This structure connecting these different regions with the help of a throat is called the Einstein-Rosen bridge. However, the throat tends to collapse and the model is reduced to a black hole. Morris and Thorne [38] showed that if effective matter in the throat is an exotic matter with negative pressure, the wormhole could have a stable throat due to repulsive effects of the matter. With this idea of a traversable and stable structure, many remarkable topics such as interuniverse transition, time-machine, space-time travel are taken into consideration together with wormholes [39]. The fact that wormholes are bridges that allow travel in space, time or space-time causes this phenomenon to be primarily investigated in both General Relativity and other alternative gravitation theories. On the other hand, symmetries are a way to simplify mathematical language used to describe and understand events and systems. For example, axial symmetries, spherical symmetries, mirror symmetries and inheritance symmetries [40]. In addition, the symmetries of space-time geometries contribute positively to the solvability of difficult-to-solve systems such as Einstein field equations. Such systems can be described by means of isometries . Some useful constraints can be applied to the space-time geometry by means of Killing vectors, and especially gauged conformal Killing vectors [41]. Kuhfitting [42], proposed a traversable wormhole model that allows the one-parameter group of conformal motion with barotropic equation of state. In recent years, wormhole models with symmetry along conformal Killing vectors have been widely investigated in alternative gravitation theories. Under the leadership of all these studies, our main motivation in this study is to obtain conformal wormholes from perspective of $f(R, \mathfrak{L}_m)$ theory, to discuss stability conditions of constructed model in geometric and dynamic aspects and to define matter and/or energy field that could be source of such wormholes.

The content of the study is as follows: Field equations and related connection of $f(R, \mathfrak{L}_m)$ theory, wormhole geometry and geometrical stability conditions are mentioned in section 2. In section 3, wormhole space-time was reconstructed under conformal symmetry. Redshift function and shape function of the wormholes were defined under the conformal symmetry. In the framework of $f(R, \mathfrak{L}_m)$ gravity, field equations and their solutions were obtained for conformal wormholes with anisotropic distribution. Geometric traversability and stability conditions of the conformal wormholes were obtained in section 4. Traversability and stability properties of conformal wormholes were revealed dynamically with the help of energy conditions in section 5. Obtained results, literature comparisons and important findings are summarized and discussed in section 6.

2. $f(R, \mathfrak{L}_m)$ theory and wormholes

If it is desired to present matter-geometry relation under a function with an alternative approach directly in Einstein-Hilbert action, and if the matter-geometry coupling and Lagrangian density of matter are accepted to vary only according to metric potentials, such a gravitational theory is represented by an action integral as follows:

$$S = \int f(R, \mathfrak{L}_m)\sqrt{-g}\,d^4x \tag{1}$$

where $f(R, \mathfrak{L}_m)$ is determining function of the theory [24]. R and $\mathfrak{L}_m$ sign Ricci scalar and Lagrangian density of matter, respectively [24]. In accordance with least action principle, field equations of the theory, which reveal coupling of matter-geometry are obtained from variation of equation (1) as follows:

$$f_R R_{ik} + (g_{ik}\,\Box - \nabla_i\nabla_k)f_R - \frac{1}{2}(f - f_{\mathfrak{L}_m}\mathfrak{L}_m)g_{ik} = \frac{1}{2}f_{\mathfrak{L}_m}T_{ik} \tag{2}$$

where $f_R = \frac{\partial f}{\partial R}$, $f_{\mathfrak{L}_m} = \frac{\partial f}{\partial \mathfrak{L}_m}$ and $f = f(R, \mathfrak{L}_m)$ [24]. Also, ∇_i and $\Box$ symbolize covariant derivative and d'Alambertian operator, respectively. T_{ik} characterizes stress-energy tensor of matter. The tensor is given as depend on Lagrangian density of matter and metric potentials by [43]:

$$T_{ik} = -\frac{2}{\sqrt{-g}}\frac{\delta(\sqrt{-g}\,\mathfrak{L}_m)}{\delta g^{ik}}. \tag{3}$$

By considering contraction of field equations given by equation (2), one gets trace of second rank tensors defined on the right and left sides of the equation provides an additional equation from which $f(R, \mathfrak{L}_m)$ can be isolated:

$$Rf_R + 3\,\Box f_R - 2(f - f_{\mathfrak{L}_m}\mathfrak{L}_m) = \frac{1}{2}f_{\mathfrak{L}_m}T. \tag{4}$$

In addition, conservation of energy and momentum in the theory are defined with covariant derivative of field equations by Harko and Lobo [24]:

$$\nabla_i T_{ik} = 2\nabla_i \log(f_{\mathfrak{L}_m})\frac{\partial \mathfrak{L}_m}{\partial g^{ik}}. \tag{5}$$

Wormhole geometries appertain two serious functions which directly affect structural properties of the formations: redshift function $\Phi(r)$ and shape function $b(r)$. They are defined by following line element as Einstein-Rosen bridge on eliminating singularities of black holes [44]:

$$ds^2 = e^{\Phi(r)}dt^2 - \left(1 - \frac{b(r)}{r}\right)^{-1}dr^2 - r^2d\theta^2 - r^2\sin^2\theta d\Phi^2. \tag{6}$$

Wormholes provide infrastructure with openings to separate manifolds. Therefore, in addition to associating different space-time parts, it could also offer opportunity to transition between these regions. A wormhole can be unstable and collapsing like a black hole, or it can be stable and traversable. Traversability properties of wormholes are determined by boundary conditions of redshift and shape functions [38].

- Condition associated with redshift function limits coherent motion of the wormhole with expanding universe and limits its stable structure by avoiding singularities. The function must be finite along radial coordinate [45].
- Since shape function directly determines throat radius of the wormhole (r_0), the conditions which restrict shape function of being traversable, ensure non-collapsing and singularity-free wormholes [45]:
  - (i) throat radius condition: $b(r) = r_0$ at $r = r_0$,
  - (ii) throat condition: $b(r) < r$ at $r_0 < r < \infty$,
  - (iii) flare-out condition: $\frac{db(r)}{dr} < 1$ at $r_0 < r < \infty$,
  - (iv) asymptotically flatness condition: $b(r)/r \to 0$ at $r \to \infty$,
  - (v) proper distance condition: $\left|\int_{r_0}^{r}\frac{dr}{\sqrt{\frac{r-b(r)}{r}}}\right| \geqslant r - r_0$ for all asymptotical regions.

3. Conformal wormholes in $f(R, \mathfrak{L}_m)$ theory

The geometrical structure commonly used in star models is spherical symmetry, and the most suitable effective matter of star is considered to be anisotropic fluid due to its properties such as electromagnetic effects and rotation. On the other hand, anisotropic distributions are at the forefront in modeling phenomena with high mass density such as compact objects, black holes, exotic stars [46]. Although there are isotropic solutions at the Planck scale level for the physical construction of wormholes, this model is not a geometric infrastructure that can only be produced by gravity [47]. Wormholes are taken into consideration not only from a quantum perspective, but also from a simple anisotropic structure within the framework of General Relativity or alternative gravity theories [48]. In order that wormhole throat to meet traversability conditions, it must first

Table 1. Type of vector field of symmetry according to conformal factor.

Vector field of conformal symmetry	Conformal factor
Killing Vectors	$\psi = 0$
Homothetic Killing Vectors	$\psi_{,i} = 0$ and $\psi \neq 0$
Special Conformal Killing Vectors	$\psi_{,ik} = 0$, $\psi_{,i} \neq 0$ and $\psi \neq 0$
non-Special Conformal Killing Vectors	$\psi_{,ik} \neq 0$, $\psi_{,i} \neq 0$ and $\psi \neq 0$

have an initial value other than zero. This geometrical result could only be achieved if effective matter has negative pressure and radial/tangential effects are observed. For this reason, source of the wormholes is commonly considered to be an anisotropic fluid. Energy-momentum tensor is given by

$$T_{ik} = (\rho + p_t)u_i u_k - p_t g_{ik} + (p_r - p_t)x_i x_k \tag{7}$$

where $\rho(r)$, $p_r(r)$ and $p_t(r)$ are energy density, radial and tangential pressure of the fluid, respectively. u_i and x_i sign four-velocity and unit four-vector. By considering equations (2), (6) and (7), field equations for wormholes are attained in $f(R, \mathfrak{L}_m)$ theory as follows:

$$4f'_R\left(\frac{r-b}{r^2}\right) + 2f_R\left(\frac{b'r-b}{r^3}\right) - (f - f_{\mathfrak{L}_m}\mathfrak{L}_m) = f_{\mathfrak{L}_m}p_r, \tag{8}$$

$$2f''_R\left(\frac{r-b}{r}\right) + f'_R\left(\frac{2r-b-b'r}{r^2}\right) + f_R\left(\frac{b'r+b}{r^3}\right) - (f - f_{\mathfrak{L}_m}\mathfrak{L}_m) = f_{\mathfrak{L}_m}p_t \tag{9}$$

and

$$2f''_R\left(\frac{r-b}{r}\right) - f'_R\left(\frac{4r+3b+b'r}{r^2}\right) - (f - f_{\mathfrak{L}_m}\mathfrak{L}_m) = f_{\mathfrak{L}_m}\rho \tag{10}$$

where prime symbolizes derivative with respect to radial coordinate. It is considered that four velocity is suitable for co-moving movement and unit four-vector is in the radial direction.

Static spherically symmetric space-times satisfy conformal symmetry throughout vector field such as $\xi^a \equiv (\xi^1, 0, 0, \xi^4) \equiv (\frac{r\psi(r)}{2}, 0, 0, c_1)$ where $\psi(r)$ represents conformal factor and c_1 is integration constant [45]. Properties of conformal factor could be understood from solutions of $\mathfrak{J}_\xi g_{ik} \equiv \psi(x^a)g_{ik} \equiv \xi_{i;k} + \xi_{k;i}$ and field equation, which determine symmetry. Table 1 summarizes vector fields of the symmetry and function properties of the conformal factor [49]:

Similarly, wormhole geometry with conformal symmetry is obtained by subjecting the metric potentials given in equation (6) to Lie derivative along the same ξ^a vector field as follows:

$$e^{\Phi(r)} = c_2^2 r^2, \tag{11}$$

$$\left(1 - \frac{b(r)}{r}\right)^{-1} = \frac{c_3^2}{\psi^2(r)}, \tag{12}$$

$$\xi^a = c_1\delta^a_4 + \frac{r\psi(r)}{2}\delta^a_1. \tag{13}$$

Spherically symmetric space-time which has conformal symmetry can be written as

$$ds^2 = -c_2^2 r^2 dt^2 + \frac{c_3^2}{\psi^2(r)}dr^2 + r^2 d\theta^2 + r^2\sin^2\theta d\phi^2 \tag{14}$$

where c_2 and c_3 are integration constants [50].

According to nature of the fluid dynamics, matter Lagrangian $\mathfrak{L}_m$ can be expressed depending on the dynamic components of the fluid. This expression is $\mathfrak{L}_m \equiv \mathfrak{L}_m(\rho, p)$ in general form [24]. With equation of state ($p = \omega\rho$), pressure of the fluid can be expressed as a function of its energy density such as $p(\rho)$. Similarly, with another preference, the energy density can be used as a function of pressure such as $\rho(p)$. Therefore, the matter Lagrangian can also be chosen as a function of pressure only $\mathfrak{L}_m(p)$ or as a function of energy density only $\mathfrak{L}_m(\rho)$. There are many examples that try to clarify different cosmological and gravitational problems using simple functions of both cases. The nature of these choices is discussed in detail in [24]. In this study, we prefer the choice that allows us to compare with existing studies and is widely used in the literature [51–53]:

$$\mathfrak{L}_m = \rho(r). \tag{15}$$

Let us take into consideration $\mathfrak{L}_m$ model, which can be easily reduced to Einstein gravity with cosmological constant and is defined as directly responsible for gravitational field:

$$f(R, \mathfrak{L}_m) = \frac{R}{2} + n\mathfrak{L}_m^{\alpha} + \beta \tag{16}$$

where n, α and β are constants related with dimensional coupling, field contribution and expansional structure, respectively [24, 54–58].

An exotic matter source with negative pressure is needed to prevent throat radius of wormholes from approaching to zero. In modified gravity theories, extra contributions in Einstein-Hilbert action change effect of matter. Therefore, it is clear that proportionality coefficient in equation of State (EoS) is negative for effective matter, but can be either positive or negative for fluid matter. Therefore, under mentioned considerations and condition $p_r(r) = \omega\rho(r)$, field equations given by equations (8)–(10) are obtained as follows:

$$\frac{6\psi^2}{c_3^2 r^2} - \frac{2}{r^2} - 2\beta = 2\rho^{\alpha}(\alpha(\omega - 1) + n), \tag{17}$$

$$\frac{4\psi'\psi}{c_3^2 r} + \frac{2\psi^2}{c_3^2 r^2} - 2\beta = 2\rho^{\alpha}\left(\frac{\alpha}{\rho}(p_t - \rho) + n\right) \tag{18}$$

and

$$\frac{4\psi'\psi}{c_3^2 r} + \frac{2\psi^2}{c_3^2 r^2} - \frac{2}{r^2} - 2\beta = 2\rho^{\alpha}(n - 2\alpha). \tag{19}$$

From equations (17)–(19), we get exact solutions of the field equations in the following form:

$$\psi(r) = \left(\frac{c_3^2\beta r^2}{3} + c_4 r^{-\frac{\alpha\omega+5\alpha-2}{\alpha\omega-\alpha+1}} + \frac{\alpha c_3^2(\omega+1)}{\alpha\omega+5\alpha-2}\right)^{\frac{1}{2}}, \tag{20}$$

$$\rho(r) = \left(\frac{3c_4(\alpha(\omega+5)-2)r^{\frac{2-\alpha(\omega+5)}{1+\alpha(\omega-1)}} + 2c_3^2(\alpha(\omega-1)+1)}{r^2 c_3^2(\alpha(\omega+5)-2)(\alpha(\omega-1)+1)}\right)^{\frac{1}{\alpha}}, \tag{21}$$

$$p_r(r) = \omega\left(\frac{3c_4(\alpha(\omega+5)-2)r^{\frac{2-\alpha(\omega+5)}{1+\alpha(\omega-1)}} + 2c_3^2(\alpha(\omega-1)+1)}{r^2 c_3^2(\alpha(\omega+5)-2)(\alpha(\omega-1)+1)}\right)^{\frac{1}{\alpha}} \tag{22}$$

and

$$\begin{aligned} p_t(r) = -\frac{1}{\alpha}&\left(\frac{3c_4(\alpha(\omega+5)-2)r^{\frac{2-\alpha(\omega+5)}{1+\alpha(\omega-1)}} + 2c_3^2(\alpha(\omega-1)+1)}{r^2 c_3^2(\alpha(\omega+5)-2)(\alpha(\omega-1)+1)}\right)^{\frac{1}{\alpha}} \\ &\left(c_4(\alpha(\omega+5)-2)r^{\frac{2-\alpha(\omega+5)}{1+\alpha(\omega-1)}} + 2\frac{c_3^2}{3}(\alpha(\omega-1)+1)\right)^{-1} \\ &\left(c_4\alpha(\alpha(\omega+5)-2)r^{\frac{2-\alpha(\omega+5)}{1+\alpha(\omega-1)}} - \frac{c_3^2}{3}(\alpha(\omega+3)-2)(1+(\omega-1)\alpha)\right) \end{aligned} \tag{23}$$

where c_4 is arbitrary constant. Also, dimensional coupling constant n is unitized and selected as $n = 1$.

Within the framework of $\mathfrak{L}_m$ theory, energy density obtained in equation (21) for anisotropic fluid that creates obtained wormhole geometry is given in figure 1. It can be seen that solution has a singularity in the case of $p_r = -\rho$. It is clear that energy density takes positive values in the range of $\omega < -1$ or $\omega > -1$. Additionally, it is seen to have maximum values near $\omega \to -1$ neighborhoods around r $\to r_0$. However, when $r \to \infty$, it approaches $\rho|_{r\to\infty} \to 0$. In the neighborhoods of $r \to r_0$, ρ becomes zero for $\omega \ll -1$ or $\omega \gg -1$.

Change of radial pressure for the constructed model is given in figure 2. Singularity at $\omega = -1$ is also clearly seen in the change of p_r function. Figure 2(a) is obtained for positive ω values and figure 2(b) is obtained for negative ω values. Since energy density is always positive, radial pressure can take positive or negative values in accordance with EoS. Therefore, constructed solution can be produced by both a normal source with positive density and pressure and/or an exotic source with negative pressure. An interesting finding from figure 1 and figure 2 is that the source distribution is very concentrated around throat of constructed model. While the source effect is seen in neighborhoods smaller than throat radius, this effect disappears quickly as the radius increases. Tangential pressure of the solution is given in figure 3. Although it appears to be different from radial pressure in function, its changes with radial coordinates have a similar tendency for the region of negative radial pressure. It can be seen that the tangential pressure is negative for all values of ω, without any EoS constraint.

In this study, the singularity of the EoS parameter ω is discussed in detail for reasonable constant choices. Another factor that can singularize dynamical components of the fluid which supports the traversable and conformal wormhole structure given in equations (21) and (23) is the parameter α, which directly affects contribution of $f(R, \mathfrak{L}_m)$ gravity. As is clear from equations (21) and (23), the value $\alpha = 0$ forms the asymptote

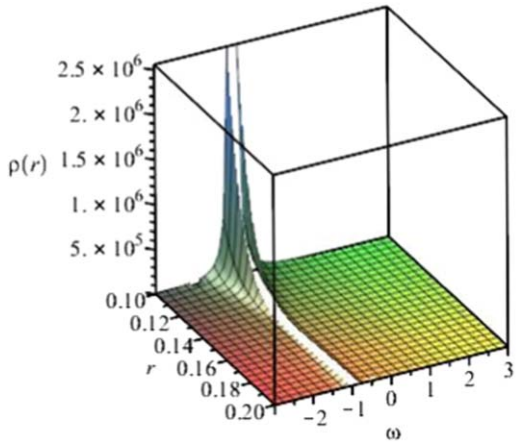

Figure 1. Energy density for the source of constructed wormholes ($c_3 = 100$, $c_4 = -1000$, $\alpha = 1/2$, $\beta = 1/1000$).

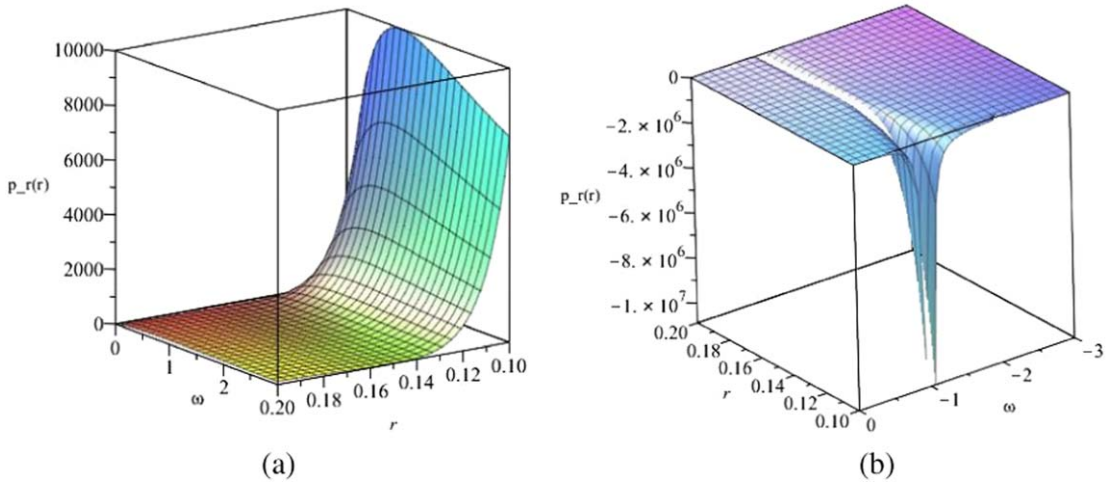

Figure 2. Radial pressure for the source of constructed wormholes ($c_3 = 100$, $c_4 = -1000$, $\alpha = 1/2$, $\beta = 1/1000$).

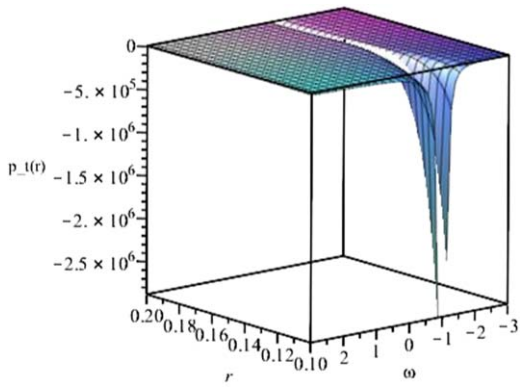

Figure 3. Tangential pressure for the source of constructed wormholes ($c_3 = 100$, $c_4 = -1000$, $\alpha = 1/2$, $\beta = 1/1000$).

for all dynamical components. As can be seen from equation (16), $\alpha = 0$ value eliminates the dependence of the matter Lagrangian on $f(R, \mathfrak{L}_m)$ model. In other words, it is not compatible with the nature of the $f(R, \mathfrak{L}_m)$ gravity approach. On the other hand, it is seen in euqations (21) and (23) that depending on the EoS parameter, separate singularities emerge at $\alpha_1 = n(1-\omega)^{-1}$ and $\alpha_2 = 2n(5+\omega)^{-1}$ values. For the selection of $n = 1$ and EoS parameter at $\omega = -1$, repeated roots in the form of $\alpha_{1,2} = 1/2$ appear. Therefore, it is considered as $\alpha = 1/2$ in

this study. However, it is useful to mention the critical values of this parameter, which directly affects extra force contribution of the $f(R, \mathfrak{L}_m)$ model. In case $\alpha = 1$, $f(R, \mathfrak{L}_m)$ model given in equation (16) reduces to General Relativity with cosmological constant. In the General Relativity limit, it is necessary to make adjustments to n constant for the singularity at $\omega = -1$. So, $n = 2$ or $n = -3$. When these constant choices are not taken into account, obtained energy density and radial pressure in equations (21) and(22) become negative. If $\alpha_1 = \alpha_2$ where $\omega = -1$, the parameter becomes depending on n constant such as $\alpha_{1,2}|_{\omega \to -1} = \frac{n}{2}$. For physically meaningful matter distribution and the search for wormhole effective matter, it is useful to make adjustments based on the constant n and evaluate other parameters according to this coupling constant setting to be $\rho \geqslant 0$ or to focus on the repeated roots case for $\alpha = n/2$ as considered in the study.

4. Viability and stability inspections

In order to define whether the obtained solution constructs wormhole geometry, it is firstly necessary to determine the shape function. From equations (12) and (20), shape function of constructed model is obtained as:

$$b(r) = \frac{2(2\alpha - 1)}{(\alpha(\omega + 5) - 2)} r - \frac{\beta r^3}{3} - \frac{1}{c_3^2} r^{-\frac{3(2\alpha-1)}{1+(\omega-1)\alpha}}. \tag{24}$$

Let's obtain functions related with the shape function in order to understand whether obtained solution is traversable wormhole geometry or not and to investigate its stability. By using derivative of equation (24), we get

$$b'(r) = \frac{3c_4}{c_3^2}(2\alpha - 1) r^{\frac{2-\alpha(\omega+5)}{1+\alpha(\omega-1)}} - \beta r^2 - 2\frac{2\alpha - 1}{\alpha(\omega + 5) - 2}. \tag{25}$$

Other important relations are as follows:

$$\frac{b(r)}{r} = -\frac{c_4}{c_3^2} r^{\frac{2-\alpha(\omega+5)}{1+\alpha(\omega-1)}} - \frac{\beta r^2}{3} + \frac{2(2\alpha - 1)}{\alpha(\omega + 5) - 2} \tag{26}$$

and

$$b(r) - r = -r\left(\frac{c_4}{c_3^2} r^{\frac{2-\alpha(\omega+5)}{1+\alpha(\omega-1)}} + \frac{\beta r^2}{3} + \frac{\alpha(\omega + 1)}{\alpha(\omega + 5) - 2}\right). \tag{27}$$

Shape function, which defines traversability conditions, for $r > r_0$, is in figure 4(a), its derivative according to radial coordinate is in figure 4(b), change with radial coordinate of $\frac{b(r)}{r}$ function is in figure 4(c) and $b(r) - r$ function is given in figure 4(d). It should be $b(r_0) = r_0$ as per throat radius condition. As seen in figure 4(a), for r $\to r_0$ it becomes $b(r) \to r_0$. From equation (24), according to constant selections considered here, r_0 value is calculated approximately 0.999. As seen in figure 4(a), shape function increases faster in all radius larger than r_0. Therefore, throat stability condition is met. On the other hand, it can be seen from figure 4(b) that derivative of the function is decreasing and its initial value is $b'(r_0) \cong 0.1$. It tends to satisfy $b'(r) < 1$ condition at all other distances. As seen in figure 4(c), $\frac{b(r)}{r}$ function is also decreasing. At the limit values of the radial coordinate and in neighborhoods far from r_0, this function also approaches to zero. Therefore, flare-out condition is also satisfied. On the other hand, if throat radius condition is satisfied, this should be clearly understood from the $b(r) - r$ function. In figure 4(d), it is clear that there is $b(r) - r|_{r \to r_0} \to 0$ and this function is negative at $r > r_0$ values. Since $b(r) < r$ at $r > r_0$ is satisfied, $b(r) - r|_{r > r_0} < 0$ is an expected condition and is provided for the obtained wormhole geometry as seen in figure 4(d).

As can be seen, since obtained solutions supply required conditions, it is revealed that constructed geometrical and dynamical structure is a traversable and conformally symmetric wormhole and that $f(R, \mathfrak{L}_m)$ theory allows these structures.

5. Energy conditions and dynamical inspections

Types of energy bounds restrict cosmological matters and/or fields. On the other hand, it also determines their properties. These bounds are used to determine physical acceptability of wormholes [59]–[62]. In this study, we take into account null, weak, dominant and strong energy conditions (NEC, WEC, DEC and SEC, respectively), which are determining conditions in investigating effects of matter-geometry couplings on each other. NEC leads that sum of the density and pressure cannot be negative, anywhere. The situation is related to the gravitational effect of obtained matter distribution. From equations (21)–(23), we get

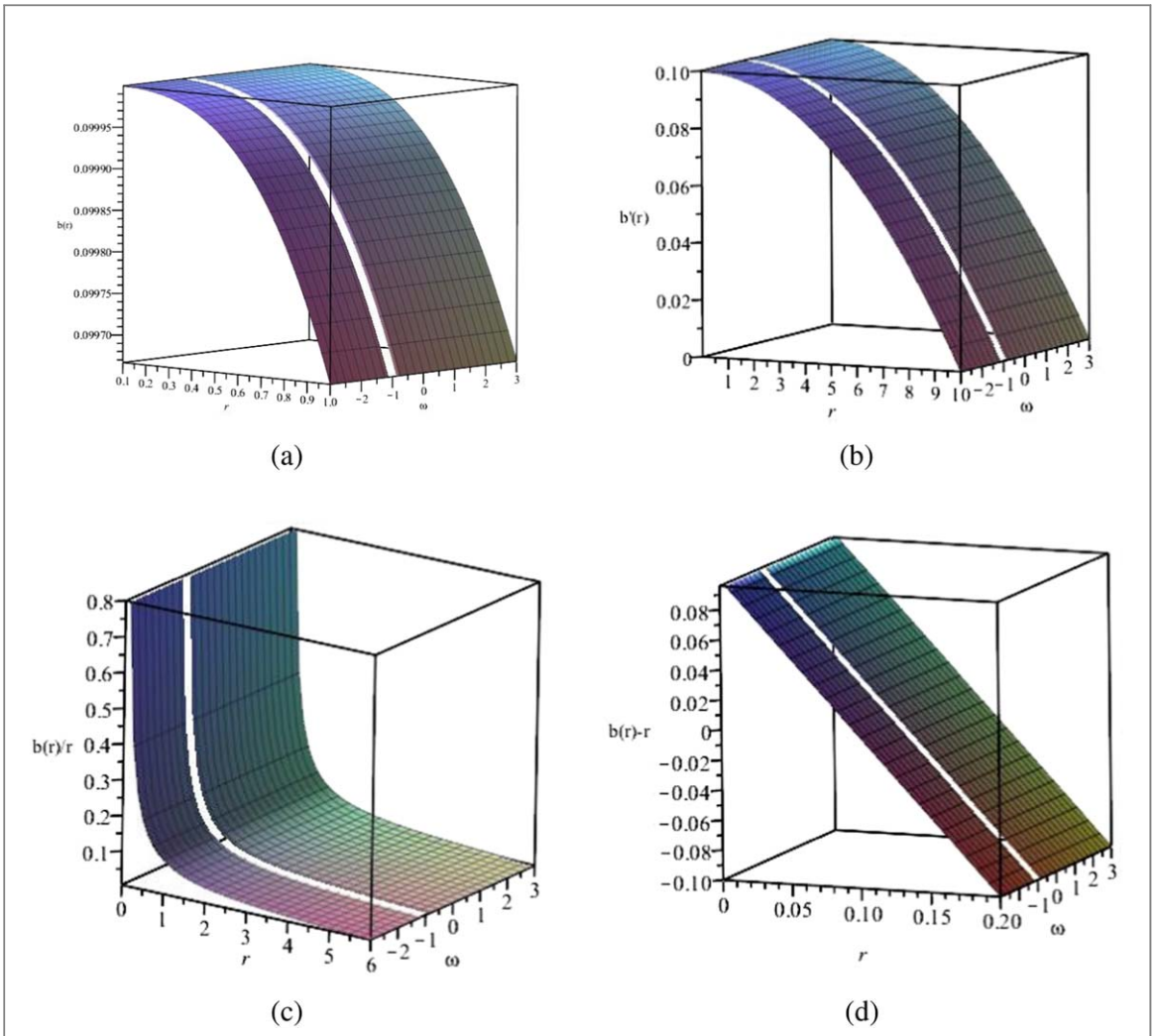

Figure 4. (a) Shape function, (b) Derivative of shape function, (c) $\frac{b(r)}{r}$ function, (d) $b(r)-r$ function, ($c_3=100, c_4=-1000, \alpha=1/2, \beta=1/1000$).

$$\rho+p_r=(1+\omega)\left(\frac{3c_4(\alpha(\omega+5)-2)r^{\frac{2-\alpha(\omega+5)}{1+\alpha(\omega-1)}}+2c_3^2(\alpha(\omega-1)+1)}{r^2c_3^2(\alpha(\omega+5)-2)(\alpha(\omega-1)+1)}\right)^{\frac{1}{\alpha}}\geqslant 0, \tag{28}$$

$$\rho+p_t=\frac{r^{-\frac{2}{\alpha}}}{\alpha}\left(\frac{3c_4(\alpha(\omega+5)-2)r^{\frac{2-\alpha(\omega+5)}{1+\alpha(\omega-1)}}+2c_3^2(\alpha(\omega-1)+1)}{c_3^2(\alpha(\omega+5)-2)(\alpha(\omega-1)+1)}\right)^{\frac{1}{\alpha}-1}\geqslant 0. \tag{29}$$

In addition to NEC constraint, another condition of WEC is defined from equation (21), which states that energy density can never have negative values:

$$\rho=\left(\frac{3c_4(\alpha(\omega+5)-2)r^{\frac{2-\alpha(\omega+5)}{1+\alpha(\omega-1)}}+2c_3^2(\alpha(\omega-1)+1)}{r^2c_3^2(\alpha(\omega+5)-2)(\alpha(\omega-1)+1)}\right)^{\frac{1}{\alpha}}\geqslant 0. \tag{30}$$

DEC states that maximum interaction speed can be as fast as speed of light and that energy transfer cannot be faster. This condition is obtained from equations (21)–(23) for constructed model as follows:

$$\rho-p_r=(1-\omega)\left(\frac{3c_4(\alpha(\omega+5)-2)r^{\frac{2-\alpha(\omega+5)}{1+\alpha(\omega-1)}}+2c_3^2(\alpha(\omega-1)+1)}{r^2c_3^2(\alpha(\omega+5)-2)(\alpha(\omega-1)+1)}\right)^{\frac{1}{\alpha}}\geqslant 0, \tag{31}$$

$$\rho-p_t=\frac{1}{\alpha}\frac{(3c_4(\alpha(\omega+5)-2)r^{\frac{2-\alpha(\omega+5)}{1+\alpha(\omega-1)}})^{\frac{1}{\alpha}-1}}{(c_3^2r^2(\alpha(\omega+5)-2)(1+\alpha(\omega-1)))^{\frac{1}{\alpha}}}$$
$$(6c_4\alpha(\alpha(\omega+5)-2)r^{\frac{2-\alpha(\omega+5)}{1+\alpha(\omega-1)}}-c_3^2(\alpha(\omega+1)-2)(\alpha(\omega-1)+1))\geqslant 0. \tag{32}$$

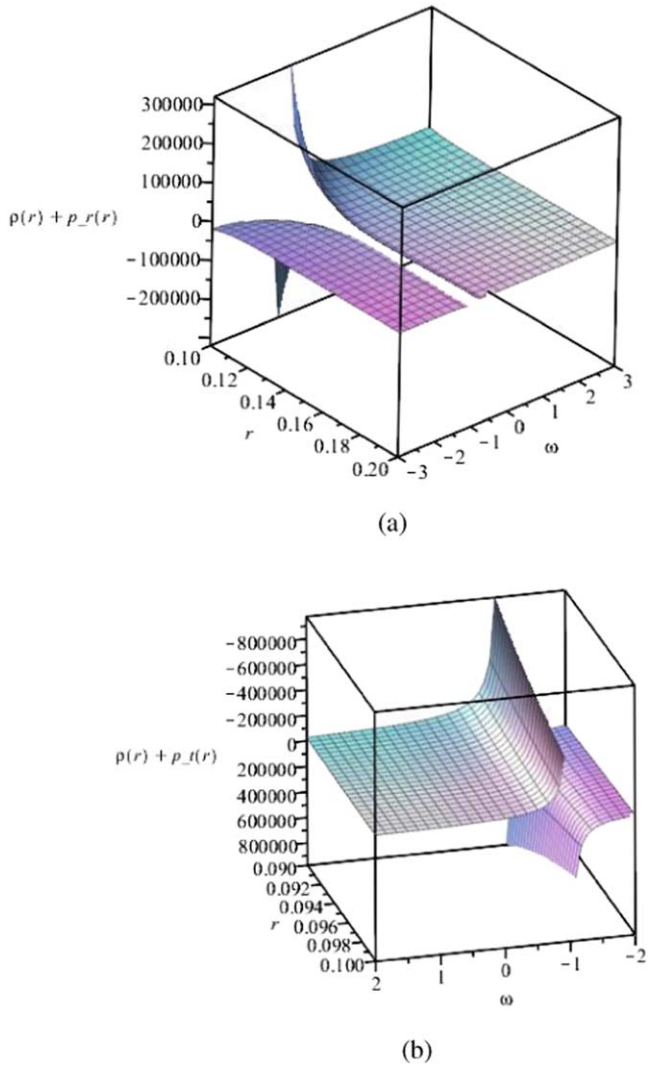

Figure 5. (a) $\rho(r)+p_r(r)$ function, (b) $\rho(r)+p_t(r)$ function, ($c_3=100, c_4=-1000, \alpha=1/2, \beta=1/1000$).

SEC also requires that trace of diagonal energy-momentum tensor is non-negative for an anisotropic matter distribution in addition to satisfying equations (28)–(29). From equations (21)–(23), we get

$$\rho + p_r + 2p_t = \frac{1}{\alpha}\frac{(3c_4(\alpha(\omega+5)-2)r^{\frac{2-\alpha(\omega+5)}{1+\alpha(\omega-1)}})^{\frac{1}{\alpha}-1}}{(c_3^2 r^2(\alpha(\omega+5)-2)(1+\alpha(\omega-1)))^{\frac{1}{\alpha}}}$$
$$(3c_4\alpha(\omega-1)(\alpha(\omega+5)-2)r^{\frac{2-\alpha(\omega+5)}{1+\alpha(\omega-1)}} - 4c_3^2(\alpha(\omega+2)-1)(\alpha(\omega-1)+1)) \geqslant 0. \quad (33)$$

Behavior of energy conditions for cases where EoS parameter is free can be seen in figure 5 - figure 7. It is clear that there is a singularity at $\omega=-1$ in energy conditions as well as in matter distributions. As seen in figure 5, sign of the values of functions changes before and after $\omega=-1$ singularity, directly. $\rho+p_r$ is negative when $\omega<-1$. However, it can be seen from figure 5(b) that $\rho+p_t$ takes positive when $\omega<-1$. This situation is exactly opposite for $\omega>-1$ in both functions. Therefore, $\rho+p_r$ violates when $\rho+p_t$ satisfies NEC, or $\rho+p_t$ violates when $\rho+p_r$ satisfies NEC. There is no at least one value of ω for which NEC is satisfied.

It can be seen in figure 1 that energy density is positive everywhere, independent from EoS parameter. Since NEC is violated, WEC is also violated even though the density is positive.

In figure 6(a), it can be seen that DEC is provided only for $\omega<-1$ values. However, for the same ω values, DEC regarding tangential pressure remains negative. Therefore, DEC is violated everywhere.

In figure 7, we see that trace function is negative for SEC at all ω values except singularity. So, SEC is violated like other conditions.

It is clear that cosmic matter and/or field in the throat of conformally symmetric $f(R, \mathfrak{L}_m)$ wormholes, which satisfies all conditions in terms of geometry, does not meet the energy conditions. The fact that no energy

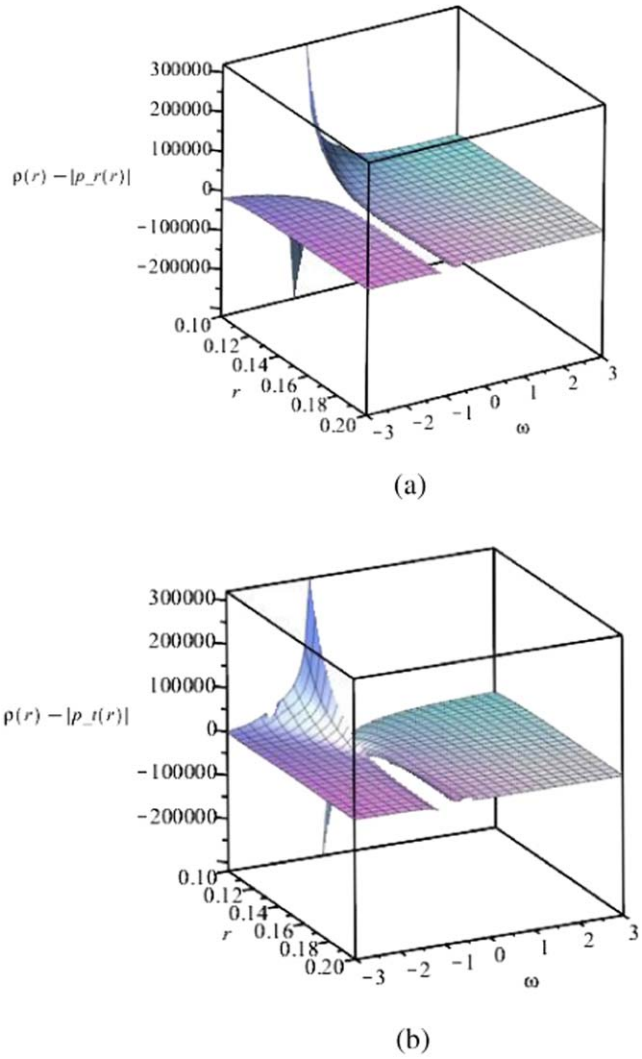

Figure 6. (a) $\rho(r) - p_r(r)$ function, (b) $\rho(r) - p_t(r)$ function, ($c_3 = 100$, $c_4 = -1000$, $\alpha = 1/2$, $\beta = 1/1000$).

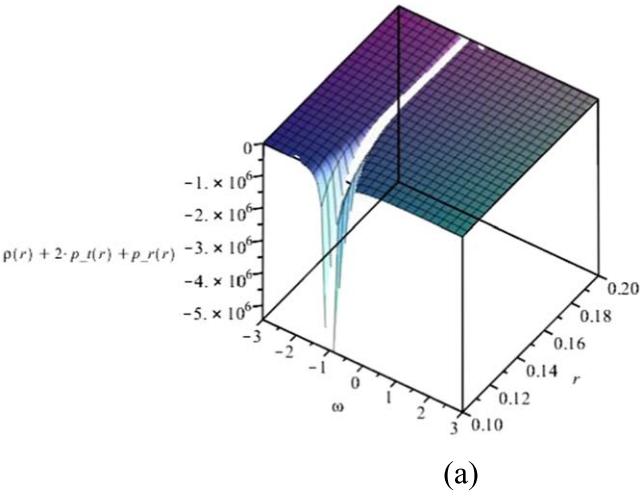

Figure 7. $\rho(r) + 2p_t(r) + p_r(r)$ function, ($c_3 = 100$, $c_4 = -1000$, $\alpha = 1/2$, $\beta = 1/1000$).

conditions are satisfied can be explained by fact that averaged energy conditions are derived from line integral and not from volume integral. At this point, the volume integral defining the averaged NEC is used. It is proposed for static spherically symmetric space-time as follows [62]:

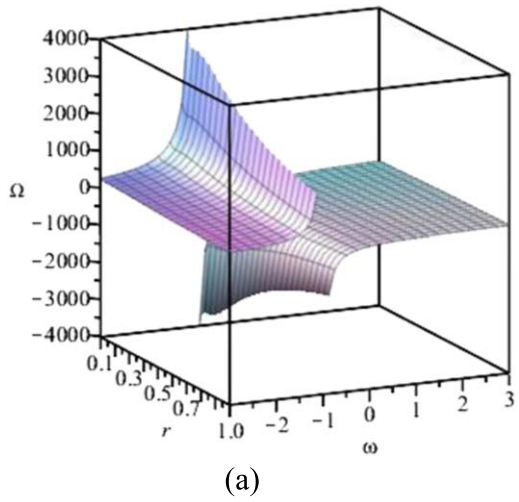

(a)

Figure 8. Volume integral ($c_3 = 100, c_4 = -1000, \alpha = 1/2, \beta = 1/1000$).

$$\Omega = \oint [\rho(r) + p_r(r)]dV$$
$$= \int_{r_0}^{\infty} 8\pi r^2(1+\omega)\left(\frac{3c_4(\alpha(\omega+5)-2)r^{\frac{2-\alpha(\omega+5)}{1+\alpha(\omega-1)}} + 2c_3^2(\alpha(\omega-1)+1)}{r^2c_3^2(\alpha(\omega+5)-2)(\alpha(\omega-1)+1)}\right)^{\frac{1}{\alpha}} dr. \tag{34}$$

Behavior of the volume integral for free EoS parameter from equation (34) and under arbitrary constant choices used in all conditions is given in figure 8. As can be seen, volume integral gives negative and positive results, with limit at singularity $\omega = -1$. This integral quantifier must be positive for physically meaningful matter distribution and energy conditions. Therefore, $\omega > -1$ values should be abandoned for conformally symmetric $f(R, \mathfrak{L}_m)$ wormholes to be physically meaningful and traversable. This situation shows us that in order for conformally symmetric $f(R, \mathfrak{L}_m)$ wormholes to be traversable, effective matter in the throat region must be an exotic matter such as phantom field.

In fact, if throat of constructed wormhole is filled with phantom field and meets traversability conditions as shown in this study, embedding diagram and geometrical pattern of this model should present open tube at the throat. With the help of cylindrical pattern relation used in proper distance condition, two-dimensional embedding diagram of proposed wormhole is obtained from equation (24) as given in figure 9.

In figure 9, $z(r)$ function becomes zero for a non-zero value of the radial coordinate. This initial value r_0 easily indicates throat radius. Three-dimensional graphics of the diagram are given in figure 10. In figure 10(a), traversation region without singularity, namely the throat, formed at radius r_0, is clearly visible. Figure 10(b) shows continuity and stable structure of the obtained conformally symmetric $f(R, \mathfrak{L}_m)$ wormholes.

Spherically symmetric structures, especially systems such as gas or fluid that are compressible and in which some interactions occur due to compression, can create a balancing pressure in the opposite direction to effect of gravitational attraction towards center. For star systems or spherically symmetric fluids, this is described by a hydrostatic equilibrium equation or Tolman-Oppenheimer-Volkoff equation [62]. For anisotropic fluid, this balance equation is defined as follows with the help of effective dynamical components:

$$-\frac{\Phi'}{2}(\rho^{eff} + p_r^{eff}) - \frac{dp_r^{eff}}{dr} + \frac{2}{r}(p_t^{eff} - p_r^{eff}) = 0. \tag{35}$$

In this study, field equations for spherically symmetric anisotropic fluid are obtained within the framework of $f(R, \mathfrak{L}_m)$ theory as given in equations (17)–(19). The effective dynamical components are obtained from equations (17) –(19) as follows:

$$\rho^{eff} = (2\alpha - 1)\rho^{\alpha} + \beta, \tag{36}$$
$$p_r^{eff} = -(\alpha - 1)\rho^{\alpha} + \alpha\rho^{\alpha-1}p_t + \beta, \tag{37}$$
$$p_t^{eff} = -(\alpha - 1)\rho^{\alpha} + \alpha\rho^{\alpha-1}p_r + \beta. \tag{38}$$

By considering equation (35) together with equations (16)–(38), we obtain equilibrium equation for constructed conformally symmetric $f(R, \mathfrak{L}_m)$ wormholes as follows:

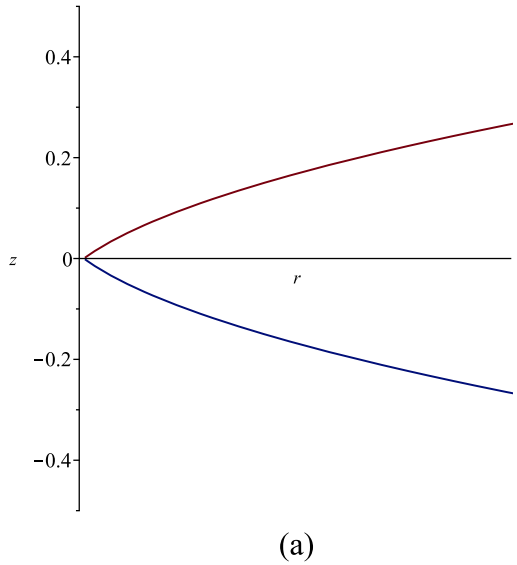

Figure 9. Proper distance of conformal $f(R,\ \mathfrak{L}_m)$ wormholes ($c_3 = 100, c_4 = -1000, \alpha = 1/2, \beta = 1/1000$).

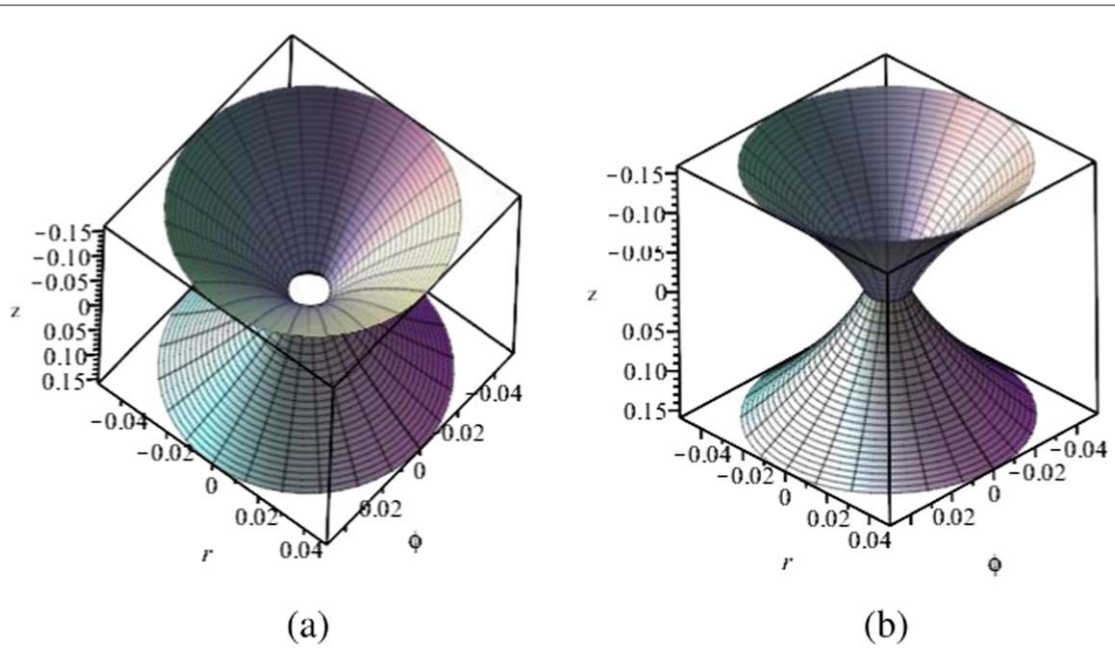

Figure 10. 3-D embedding diagram, ($c_3 = 100, c_4 = -1000, \alpha = 1/2, \beta = 1/1000$).

$$-\frac{\Phi'}{2}(\rho + p_r) - \frac{dp_r}{dr} + \frac{2}{r}(p_t - p_r) + (\alpha - 1)\left(1 - \frac{p_r}{\rho}\right)\frac{d\rho}{dr} - \frac{\Phi'\beta}{\alpha}\rho^{1-\alpha} = 0 \tag{39}$$

where $-\frac{\Phi'}{2}(\rho + p_r)$ represents gravitational force (F_g), $-\frac{dp_r}{dr}$ corresponds hydrostatical force (F_h) and $\frac{2}{r}(p_t - p_r)$ is anisotropic force (F_m). On the other hand, all other expressions on the left side of equation (39) are actually extra effects (F_e) coming from $f(R,\ \mathfrak{L}_m)$ theory. Behavior of the forces for obtained conformally symmetric $f(R,\ \mathfrak{L}_m)$ wormholes is given in figure 11. Except for hydrostatic force, it is seen that these forces take positive values, including force arising from extra contributions from modified gravity theory. Positive values of the forces express attractive effect that directs distribution towards center. Negative values indicate that force has repulsive effect radially directed outward from the center. Therefore, in obtained model, gravitational and anisotropic forces appear as attractors in accordance with stellar physics or fluid dynamics. In addition, extra force coming from modified gravity theory is also attractive. It is expected that alternative gravitational theories proposed to take over and develop role and shortcomings of cosmological constant in Einstein's theory of gravity would make an appropriate contribution to expansion of Universe. It is noteworthy that the extra contribution

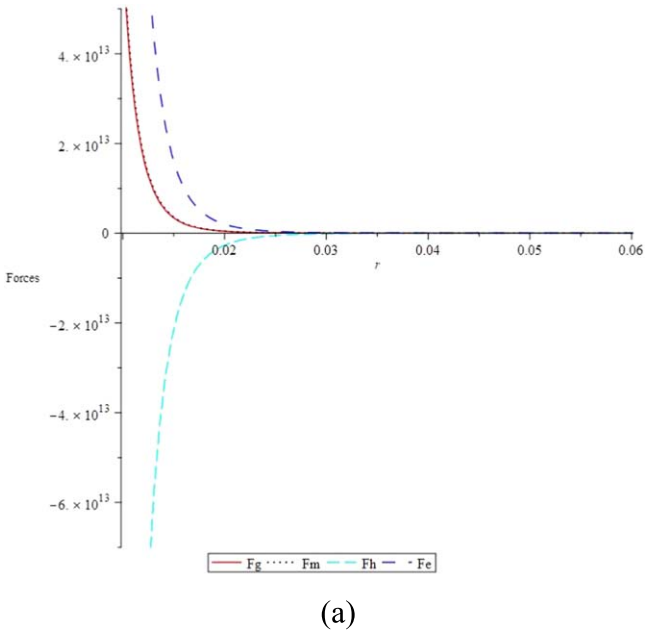

Figure 11. Forces of conformal symmetric $f(R,\ \mathfrak{L}_m)$ wormholes ($c_3 = 100, c_4 = -1000, \alpha = 1/2, \beta = 1/1000$).

obtained here exhibits attractive behavior. On the other hand, it is hydrostatic force that balances these attractive forces. It is so dominantly repulsive that it absorbs impact of all other forces from center to outside. While anisotropic factors that prevent collapse of the wormholes and ensure stability in the throat region, that is, the contribution of radial and tangential pressures, are attractive, it is seen that the force that helps to exhibit this stability is hydrostatic force. It has also been obtained from different gravitational theories that the hydrostatic force dominates for conformal wormholes [53–62].

6. Conclusion

In this study, we construct wormholes with conformal symmetry in $f(R,\ \mathfrak{L}_m)$ theory. We investigate field equations and their solutions by obtaining relationship of metric potentials with the conformal factor from symmetry properties. Field equations of $f(R,\ \mathfrak{L}_m)$ theory give a static conformally symmetric solution for anisotropic fluid distribution. From this solution, we determine shape function of the wormholes.

Dynamical components of anisotropic fluid distribution are obtained. Singularity is seen at $\omega = -1$. It is seen that anisotropic fluid filled the obtained wormholes must be candidate matters and/or fields that comply with $p_r(r) \neq -\rho(r)$ inequality. Obtained energy density is positive everywhere. For all forms that would not fall into singularity, a cosmic matter and/or field distribution with positive energy density in all cases, regardless of EoS parameter, supports constructed $f(R,\ \mathfrak{L}_m)$ wormholes with this symmetry. As expected, radial pressure takes positive values for positive EoS parameter, while it has negative values for $\omega < -1$. It is understood that tangential pressure is negative everywhere, regardless of the ω parameter. The possible values of the EoS parameter ω are decisive in the form of matter that fills space-time. For example, $\omega > 0$ state describes normal matter forms such as stiff fluid, radiation or dust. On the other hand, the EoS parameter with a negative value indicates exotic substances such as phantom energy, dark energy and quintessence matter. The inflation and recent expansion of the Universe are characterized by dark energy. As the most basic approach, there is $\omega = -1$, which corresponds to the cosmological constant. However, this sharp value is invalid for the exponential scale factor. Today's observations indicate that the EoS parameter of the cosmological constant may have a value different from -1 but close to it. Therefore, instead of the actually invalid value $\omega = -1$, dust-like dark energy $\omega > -1$ and phantom-like dark energy $\omega < -1$ can be source of inflation and recent expansions. Although a static model is taken into account in this study, as can be seen from the obtained graphs, the simple cosmological constant approach acts as a barrier within the framework of $f(R,\ \mathfrak{L}_m)$ gravity. If potential energy is zero in the fluid-scalar field coupling, the $\omega = 1$ state occurs. On the other hand, in the absence of kinetic energy, the EoS parameter is obtained as $\omega = -1$, which corresponds to the cosmological constant. Due to the dynamic structure of conformal wormholes with anisotropic fluid obtained in this study, the kinetic energy of the distribution is not expected to be zero. The $\omega = -1$ singularity, encountered in this study, indicates that generalization of $f(R,\ \mathfrak{L}_m)$ gravity is compatible with observational results and expectations. On the other hand, the appearance

of the $\omega = -1$ barrier even in a static space-time model implies the importance of considering the crossing Phantom Divide Line (PDL) investigations within the framework of $f(R, \mathfrak{L}_m)$ gravity in appropriate models in order to understand the evolution processes of dark energy from dust-like to phantom-like.

It is seen that obtained shape function meets all required viability and stability conditions, independent of EoS parameter. A real throat radius is defined. The behavior of shape function and related functions is consistent with this initial value. Energy conditions are taken into account to examine stability of resulting wormhole geometry and matter distribution that would prevent collapse in the throat region. It is seen that dynamical components of the matter distribution violate all energy conditions.

We investigate uncertainty that arises in energy conditions and physical significance of resulting matter distribution by calculating volume integral. Volume integration showed that obtained solutions are only possible in the range of $\omega < -1$. That is, in $f(R, \mathfrak{L}_m)$ theory, fluid filled the conformally symmetric wormholes must be an exotic matter such as a phantom field. This situation was encountered similarly in studies of wormholes with conformal symmetry obtained within the framework of other alternative gravitational theories [53–62].

Since all conditions are met, it is clear that anisotropic fluid distribution such as a phantom field prevents collapse in the wormhole throat. This situation is expected to be seen in embedding diagrams of the constructed model. In the embedding diagrams in two and three dimensions, it is clearly seen that $f(R, \mathfrak{L}_m)$ wormholes with conformal symmetry have a singularity-free throat and a continuous structure. In general, there are interconnecting relationships between energy conditions [64]. For example, NEC is a sub-state of WEC. WEC is a sub-condition of DEC. Independent of WEC and DEC, NEC is also a subordinate requirement within the SEC [64]. Therefore, in terms of the general classical approach, when the NEC is not met, the WEC must be automatically violated. Since NEC and WEC are not provided, DEC is also violated [64]. On the other hand, due to the violation of the NEC, there is also a violation of the SEC [64]. In this study, it is found that all energy conditions for the constructed model were violated. On the other hand, it is obtained that $\omega < -1$ is the physical significance of the constructed model. In other words, it can be seen that the effective matter of the resulting wormhole model is the phantom field. It is frequently emphasized in the literature that wormholes can have traversable properties if supported by phantom fields, both within the framework of $f(R, \mathfrak{L}_m)$ gravity and/or other gravity approaches [31, 32, 64]. However, in some of similar studies, energy conditions appear as examples where the NEC is violated and all or some of the other conditions are met or violated, without the relationships between them. Under the exotic matter approach, a phantom field would require a violation of the NEC [64]. This study, in which we obtained that all energy conditions are violated, shows that stable and traversable conformal wormholes can be a successful model that can provide the infrastructure for studies such as warp-drive or space-time travel, and supports the consistency of $f(R, \mathfrak{L}_m)$ gravity in this respect.

Another noteworthy issue is that obtained matter distribution is completely independent of β constant, which is included in determining function of $f(R, \mathfrak{L}_m)$ theory. β constant in obtained solutions, it appears as a parameter that affects metric potentials but does not contribute to dynamical components. Remarkable point here is that the constant matches cosmological constant in the General Relativity limits of $f(R, \mathfrak{L}_m)$ theory. In short, according to obtained results, exotic matter, which is source of conformally symmetric wormhole within the framework of $f(R, \mathfrak{L}_m)$ theory, cannot be associated with contribution held responsible for expansion of Universe.

Data availability statement

No new data were created or analysed in this study.

ORCID iDs

Doğukan Taşer https://orcid.org/0000-0002-8622-6830
Melis Ulu Doğru https://orcid.org/0000-0003-1788-3885

References

[1] Slipher V 1913 *Lowell Observatory Bulletin* **1** 56–7
[2] Friedman A 1922 *Zeitschrift für Physik* **10** 377–86
[3] Lemaître G 1927 *Annales de la Société Scientifique de Bruxelles* **A47** 49–59
[4] Steer I 2021 *Nature* **490** 176
[5] Baade W 1979 The resolution of Messier 32, NGC 205, and the central region of the Andromeda Nebula. *In A Source Book in Astronomy and Astrophysics* (Harvard University Press) 744–9
[6] Allen N 2001 *The Cepheid Distance Scale: A History* MSc thesis at Queen Mary College, University of London.

[7] Trauger J T 1994 *Astrophysical Journal Letters* **435** L3–6
[8] Freedman W L 1996 *Science with the Hubble Space Telescope-II II. Proceedings of a workshop held in Paris, France (Baltimore, MD: Space Telescope Science Institute)* ed P Benvenuti *et al* p 3 https://ui.adsabs.harvard.edu/abs/1996swhs.conf.....B/abstract
[9] Reiss A, Press W and Kirshner R 1995 *Astrophys.J.* **438** L17–20
[10] Spergel D N *et al* 2003 *Astrophys. J. Suppl. Ser.* **148** 175–94
[11] Riess A G *et al* 1998 *Astron. J.* **116** 1009–38
[12] Copeland E J, Sami M and Tsujikawa S 2006 *Int. J. Mod. Phys.* D **15** 1753
[13] Frieman J, Turner M and Huterer D 2008 *Ann. Rev. Astron. Astrophys* **46** 385–432
[14] Weinberg S 1989 *Rev. Mod. Phys.* **61** 1
[15] Faraoni V 2004 *Cosmology in Scalar-Tensor Gravity* (Kluwer Academic)
[16] Kobayashi T 2019 *Rep. Prog. Phys* **82** 086901
[17] Baker M R and Kuzmin S 2019 *Int. J. Mod. Phys.* D **7** 1950092
[18] Thomas R S and Valerio F 2010 *Rev. Mod. Phys.* **82** 451
[19] Harko T, Lobo F S N, Nojiri S and Odintsov S D 2011 *Phys. Rev.* D **84** 024020
[20] Ulu Doğru M, Ayd∈ H and Taşer D 2023 *Int. J. Geom. Meth. Mod. Phys.* **20** 2350073
[21] Rajabi F and Nozari K 2017 *Phys. Rev.* D **82** 084061
[22] Oikonomou V K and Chatzarakis N 2020 *Nucl. Phys. B* **956** 115023
[23] Bahamonde S, Böhmer C G, Lobo F S and Sáez-Gómez D 2015 *Universe* **1** 186–98
[24] Harko T and Lobo F S N 2010 *Eur. Phys. J.* C **70** 373–9
[25] Harko T and Lake M J 2015 *Eur. Phys. J.* C **75** 1–18
[26] Jaybhaye L V, Solanki R, Mandal S and Sahoo P K 2022 *Phys. Lett.* B **831** 137148
[27] Bertolami O, Páramos J and Turyshev S G 2008 General Theory of Relativity: Will it survive the next decade? *Lasers, Clocks and Drag Free Control: Exploration of Relativistic Gravity in Space* (Springer) 27–74
[28] Wang J and Liao K 2012 *Class. Quantum Grav.* **29** 215016
[29] Maurya D C 2023 *New Astron.* **100** 101974
[30] Jaybhaye L V, Snehasish B and Sahoo P K 2023 *Physics of the Dark Universe* **40** 101223
[31] Solanki R, Hassan Z and Sahoo P K 2023 *Chin. J. Phys.* **85** 74–88
[32] Kavya S N, Venkatesha V, Mustafa G, Sahoo P K and Rashmi S D 2023 *Chin. J. Phys.* **84** 1–11
[33] Venkatesha V, Kavya N S and Sahoo P K 2023 *Phys. Scr.* **98** 065020
[34] Dixit A, Chawla C and Pradhan A 2021 *Int. J. Geom. Meth. Mod. Phys.* **18** 2150064
[35] Chawla C, Dixit A and Pradhan A 2021 *Can. J. Phys.* **99.8** 634–45
[36] Tangphati T, Muniz C R, Pradhan A and Banerjee A 2023 *Physics of the Dark Universe* **42** 101364
[37] Pradhan A, Islam S, Zeyauddin M and Banerjee A 2023 arXiv:2310.07181
[38] Morris S M and Thorne S K 1988 *Am. J. Phys.* **56** 395–412
[39] Banerjee A, Hansraj S and Pradhan A 2024 arXiv:2402.11348
[40] Garcia N M and Lobo F S 2010 *Physical Review D* **82** 104018
[41] Tayde M, Hassan Z and Sahoo P K 2024 *Chin. J. Phys.* **89** 195–209
[42] Kuhfittig P K 2017 arXiv:1707.04150
[43] Landau L D and Lifshitz E M 2002 *The Classical Theory of Fields* (Butterworth-Heinemann)
[44] Einstein A and Rosen N 1935 *Phys. Rev.* **48** 73
[45] Herrera L and Ponce de León J 1985 *J. Math. Phys.* **26** 2018–23
[46] Ditta A, Ahmad M, Hussain I and Mustafa G 2021 *Chin. Phys.* C **45** 045102
[47] Kim H 2013 *Astropart. Phys.* **46** 50–4
[48] Sahoo P K, Moraes P H R S, Sahoo P and Ribeiro G 2018 *Int. J. Mod. Phys.* D **27** 1950004
[49] Yilmaz I, Tarhan I, Yavuz I, Baysal H and Camci U 1999 *Int. J. Mod. Phys.* D **8** 659–68
[50] Hohmann M, Pfeifer C, Raidal M and Veermae H 2018 *J. Cosmol. Astropart. Phys.* **2018** 003
[51] Bertolami O, Lobo F S N and Paramos J 2008 *Phys. Rev.* D **78** 064036
[52] Faraoni V 2009 *Phys. Rev.* D **80** 124040
[53] Brown J D 1993 *Class. Quant. Grav.* **10** 1579
[54] Pradhan A, Maurya D C, Goswami G K and Beesham A 2023 *Int. J. Geom. Meth. Mod. Phys.* **20** 2350105
[55] Maurya D C 2023 *Gravitation Cosmol.* **29** 315–25
[56] Maurya D C 2023 *Physics of the Dark Universe* **42** 101373
[57] Maurya D C 2024 *Int. J. Geom. Meth. Mod. Phys.* **21** 2450072–194
[58] Zeyauddin M, Dixit A and Pradhan A 2024 *Int. J. Geom. Meth. Mod. Phys.* **21** 2450038–144
[59] Jan M, Ashraf A, Basit A, Caliskan A and Güdekli E 2023 *Symmetry* **15** 859
[60] Singh K, Rahaman F, Deb D and Maurya S K 2023 *Frontiers in Physics* **10** 1336
[61] Naz T, Mustafa G and Shamir M F 2022 *Int. J. Geom. Meth. Mod. Phys.* **19** 2250100
[62] Sahoo P, Kirschner A and Sahoo P 2019 *Mod. Phys. Lett.* A **34** 1950303
[63] Bhar P, Rahaman F, Manna T and Banerjee A 2016 *European Physical Journal C* **76** 1–9
[64] Maeda H 2022 *Classical Quantum Gravity* **39** 075027